Acta Crystallographica Section D
Biological Crystallography
ISSN 0907-4449

Purification and crystallization of *Escherichia coli* oligoribonuclease

Tristan J. Fiedler, Helen A. Vincent, Yuhong Zuo, Orit Gavrialov‡ and Arun Malhotra*

Department of Biochemistry and Molecular Biology, University of Miami School of Medicine, PO Box 016129, Miami, FL 33101-6129, USA

‡ Current address: Department of Pediatrics, Albert Einstein College of Medicine, 1410 Pelham Parkway South, Bronx, NY 10461, USA.

Correspondence e-mail: malhotra@miami.edu

Received 7 February 2003
Accepted 27 January 2004

Oligoribonuclease (Orn) is an essential 3′-to-5′ hydrolytic exoribonuclease which degrades short oligoribonucleotides to 5′ mononucleotides. *Escherichia coli* Orn has been crystallized under several different conditions using ammonium sulfate, sodium citrate and sodium acetate as precipitants. Both native and selenomethionine-labeled oligoribonuclease (SeMet-Orn) can be crystallized at room temperature in 1.4–1.55 *M* sodium citrate. The SeMet-Orn crystals diffract to 2.2 Å resolution and belong to space group $P2_12_12_1$, with unit-cell parameters $a = 70.43$, $b = 72.87$, $c = 147.76$ Å, and two dimers in the asymmetric unit. When grown in the presence of manganese, a second crystal form (Mn-SeMet-Orn) was obtained containing a single dimer per asymmetric unit ($P2_12_12_1$; $a = 63.74$, $b = 74.31$, $c = 74.19$ Å). Finally, a hexagonal crystal form was obtained using sodium acetate as a precipitant ($a = 91.5$, $b = 91.5$, $c = 111.1$ Å). This crystal (Zn-ApUp-Orn) belongs to the $P6_5$ space group and has three oligoribonuclease molecules per asymmetric unit.

1. Introduction

RNA metabolism is dependent on exo- and endoribonucleases which together regulate a variety of cellular events including deadenylation and decay of mRNA, end turnover and 3′ processing of tRNA and maturation of ribosomal and mitochondrial RNAs. Nearly 20 RNases have been identified in *Escherichia coli*, of which eight are 3′-to-5′ exoribonucleases (reviewed in Deutscher & Li, 2001). These eight enzymes are distributed in four superfamilies and may be the complete roster of exoribonucleases in this bacterium (Zuo & Deutscher, 2001).

A steady-state concentration of mRNA is a critical component of gene expression. Disregulation of mRNA half-life can lead to pathologies including inflammation, Alzheimer's disease and cancer (Hollams *et al.*, 2002). In *E. coli*, mRNA is degraded by endo- and exoribonucleases (reviewed in Carpousis *et al.*, 1999). The endoribonucleolytic activity of RNase E is thought to initiate the process (reviewed in Coburn & Mackie, 1999), although this is still under debate (Kennell, 2002). Subsequently, the 3′-to-5′ exoribonuclease activities of RNase II and polynucleotide phosphorylase participate in mRNA decay (Deutscher, 1993). Indeed, double-mutant strains deficient in these two enzymes are inviable, accumulating mRNA fragments of 100–1500 nucleotides in length (Donovan & Kushner, 1986).

The final degradation of short oligoribonucleotides is carried out by oligoribonuclease (Orn; Ghosh & Deutscher, 1999). Orn has been shown to be a distinct 3′-to-5′ hydrolytic exoribonuclease encoded by the *orn* gene (Yu & Deutscher, 1995; Zhang *et al.*, 1998). The enzyme is a member of a larger exonuclease superfamily that includes proteins such as DNA pol III (ε subunit) and RNase T. Members of this superfamily possess the 'DEDD' motif comprised of four acidic residues distributed in three conserved regions of the primary structure (Zuo & Deutscher, 2001; Bateman *et al.*, 2002). The available DEDD exonuclease crystal structures of DNA pol I (reviewed in Steitz, 1999), pol III ε (Hamdan *et al.*, 2002) and DNA exonuclease I (Breyer & Matthews, 2000) suggest that a two metal-ion mechanism for the 3′-to-5′ exonuclease activity also occurs in Orn.

Orthologs of Orn have been identified in a broad range of organisms (Zhang *et al.*, 1998; Zuo & Deutscher, 2001), including yeast and humans (Nguyen *et al.*, 2000). Furthermore, the sequence identity between Orn orthologs in *E. coli* and *Caenorhabditis elegans* approaches 50%, which is one of the most highly conserved protein pairs in these two organisms. Indeed, this high degree of sequence identity also extends to human and murine orthologs, suggesting a critical conserved function (Koonin, 1997).

Of the eight exoribonucleases in *E. coli*, only Orn has been shown to be required for cell

viability (Ghosh & Deutscher, 1999). The enzyme is a thermostable homodimer comprised of two 20.7 kDa subunits (Zhang *et al.*, 1998). It is stimulated by Mn^{2+} and processively hydrolyses oligoribonucleotides to 5′-ribonucleotides with a reaction rate that is inversely proportional to the chain length for substrates of the form $(pA)_n$ where n is two to five nucleotides (Datta & Niyogi, 1975). Although the initial studies by Datta & Niyogi (1975) did not detect any hydrolytic activity on deoxyoligoribonucleotides of the type $d(pA)_{3–6}$, recent experiments on both *E. coli* Orn (Yuhong Zuo, unpublished results) and the human ortholog, small fragment nuclease (Nguyen *et al.*, 2000), indicate significant DNase activity.

To obtain a better understanding of their mechanism and substrate specificity, our laboratory has initiated structural studies of several DEDD exoribonucleases. Here, we present the preliminary X-ray characterization of Orn from *E. coli*. The determination of exoribonuclease crystal structures is essential for understanding both their catalytic mechanism and their ability to discriminate between DNA and RNA as well as between various RNA substrates. Furthermore, since several of the *E. coli* exoribonucleases are dimeric, high-resolution crystal structures will provide insight into the role of dimerization as it relates to either substrate binding or catalysis.

2. Material and methods

2.1. Protein expression and purification

The full-length *orn* gene from the *E. coli* genomic library of Kohara *et al.* (1987) was cloned into the high copy number vector pUC19 using the *Xba*I and *Kpn*I restriction sites (Zhang *et al.*, 1998). The resulting plasmid (pYJ19) was transformed into *E. coli* BL21 (DE3) cells that lack the Lon and OmpT proteases to facilitate protein overexpression. Transformed cells were grown in a 4 l culture of LB medium with ampicillin (100 µg ml^{-1}) for 6 h to an OD_{600} of 1.0.

Cells were harvested by centrifugation, washed in wash buffer (233 m*M* NaCl, 20 m*M* Tris pH 8.0) and frozen at 193 K. The frozen cell paste was suspended in wash buffer and lysed using a French press in the presence of protease inhibitors PMSF and pepstatin A. Polymin P [0.3%(*v*/*v*)] was used to remove DNA and most DNA-binding proteins. The Polymin P supernatant fraction was subjected to two ammonium sulfate cuts (at 1.5 and 2.5 *M*). The 2.5 *M* ammonium sulfate pellet was then dissolved in 1.5 *M* ammonium sulfate buffer with 40 m*M* Tris pH 8.0 and 150 m*M* NaCl and subsequently loaded onto a Hi-Prep phenyl Sepharose (Pharmacia Inc.) hydrophobic interaction column using an FPLC system (Pharmacia Inc.). A linear gradient of ammonium sulfate from 1.5 to 0 *M* was applied. Orn was eluted at 0.5 *M* ammonium sulfate. The fractions containing Orn were combined, dialyzed against 20 m*M* Tris pH 8.0, 75 m*M* NaCl and then applied onto a Mono Q ion-exchange column. Orn eluted from the Mono Q column at 160 m*M* NaCl during a linear gradient from 75 m*M* to 0.5 *M* NaCl. The retention time of Orn from the final Sephacryl S100 gel-filtration column (Pharmacia Inc.) was consistent with a dimeric state in solution.

The resulting protein preparation was examined by SDS–PAGE (Fig. 1) and by native PAGE, showing a single band (data not shown). Orn was concentrated to 25 mg ml^{-1} as measured by the Bradford assay (Bradford, 1976) in 20 m*M* Tris pH 8.0, 300 m*M* NaCl and 15% glycerol using Centricon-10 devices (Millipore Inc.). The protein was stored at 193 K after flash-freezing in liquid N_2 in a buffer containing 300 m*M* NaCl, 15% glycerol, 5 m*M* DTT, 1 m*M* EDTA, 20 m*M* Tris pH 8.0. All purification and concentration steps were carried out at 277 K. Typical yields of 10 mg of Orn per 4 l of culture were achieved.

SeMet-Orn was produced from the same expression vector under conditions of methionine-pathway inhibition (Van Duyne *et al.*, 1993; Doublié, 1997). Cells from a 2 ml overnight culture grown in rich medium were pelleted by centrifugation, resuspended in 10 ml M9 minimal medium containing glucose [0.4%(*w*/*v*)] and grown for 1 h at 310 K. This culture was added to 2 l of pre-warmed M9 minimal medium supplemented with the following: 0.4% glucose, 50 mg l^{-1} SeMet, 40 mg l^{-1} amino-acid set I (Ala, Arg, Asn, Asp, Cys, Glu, Gln, Gly, His, Pro, Ser), 100 mg l^{-1} amino-acid set II (Ile, Leu, Lys, Phe, Thr, Val), 40 mg l^{-1} amino-acid set III (Trp, Tyr) and 2 mg l^{-1} thiamine, thymine, niacinamide and pyridoxine monohydrochloride. The culture was grown to an OD_{600} of 0.6 at 310 K, 1 m*M* IPTG was added and the induction proceeded for 8 h. SeMet-substituted Orn was purified in a manner similar to that described above for wild-type Orn. Selenomethionine incorporation was verified by MALDI mass spectroscopy and both the wild-type and SeMet-substituted preparations were active on oligoribonucleotide substrates (data not shown).

2.2. Crystallization

Crystallization trials were carried out using the hanging-drop vapour-diffusion technique with sparse-matrix screening methods (Jancarik & Kim, 1991; Hampton Research Crystal Screens I and II) and with ammonium sulfate grid screens. Crystals of Orn grew rapidly using ammonium sulfate concentrations ranging from 2.8 to 3.2 *M*

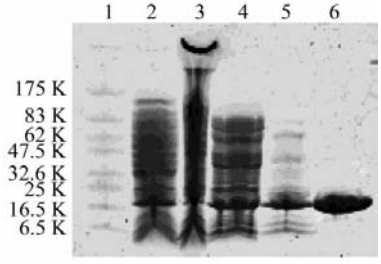

Figure 1
SDS–PAGE (8–25% Phastgel) analysis of the Orn purification procedure. Lane 1, MW standards; lane 2, cell extract; lane 3, cell extract after Polymin P step; lane 4, 2.5 *M* ammonium sulfate cut; lane 5, phenyl Sepharose column; lane 6, Mono Q column.

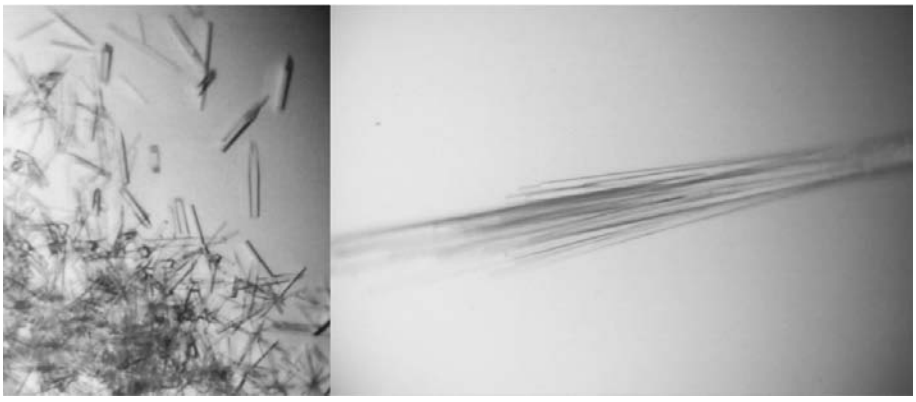

Figure 2
Orn crystals obtained with ammonium sulfate as a precipitant. The length of the crystal bundle on the right is approximately 0.8 mm.

(pH 6–8). These crystals grew in large numbers in less than 24 h and were usually small, thin and needle-like, although larger bundles nearly 1 mm in length have been observed (Fig. 2). Crystals were also obtained with condition No. 38 of Crystal Screen I (Hampton Research Inc.), which contains 1.4 *M* sodium citrate, 100 m*M* HEPES pH 7.5. Optimization of conditions gave diffraction-quality crystals grown at room temperature using 1.4–1.5 *M* sodium citrate pH 7–8 (Fig. 3).

Hexagonal crystals of oligoribonuclease (Fig. 4) were obtained at room temperature with condition No. 34 of the Crystal Screen II (Hampton Research Inc.) which contains 1.0 *M* sodium acetate, 100 m*M* HEPES pH 7.5 and 50 m*M* cadmium sulfate.

2.3. Data collection and processing

Preliminary diffraction data were collected using Cu $K\alpha$ radiation from a Rigaku RU-300 rotating-anode X-ray generator equipped with a 30 cm MAR Research image plate, an ADSC cryosystem and Supper focusing mirrors. Synchrotron diffraction data were collected on beamlines X8-C and X12-B at National Synchrotron Light Source, Brookhaven National Laboratory, which were both equipped with an ADSC Quantum Q4 area detector and an Oxford Cryostream (Fig. 5). We also collected data from the hexagonal crystal form at beamline X12-C, which is equipped with a Brandeis University B4 CCD detector. All diffraction intensities were integrated and scaled with *DENZO* and *SCALEPACK* (Otwinowski & Minor, 1997). Phase determination using multi-wavelength anomalous diffraction data was performed with *SOLVE* (Terwilliger & Berendzen, 1999; Terwilliger, 2000).

Table 1
Data-reduction and crystal parameters for oligoribonuclease crystallized in three different morphologies.

Values in parentheses are for the outermost resolution shell.

	Mn-SeMet-Orn		Zn-ApUp-Orn	SeMet-Orn		
Beamline	X12-B		X12-C	X8-C		
Crystal size (mm)	0.4 × 0.25 × 0.15		0.15 × 0.15 × 0.15	0.9 × 0.1 × 0.1		
Space group	$P2_12_12_1$		$P6_5$	$P2_12_12_1$		
Unit-cell parameters (Å)	a = 63.74, b = 74.31, c = 74.19		a = 91.55, b = 91.55, c = 111.18	a = 70.43, b = 72.87, c = 147.76		
V_M† (Å^3 Da^{-1})	2.1		2.2	2.3		
Solvent content† (%)	42		42.7	46		
Z	1 dimer		3 monomers	2 dimers		
Wavelength (Å)	0.97949	0.97887	0.97904	0.97946	0.97930	0.96411
Resolution range (Å)	50–2.0	50–2.0	50–1.7	30–2.2	30–2.2	30–2.2
Outer shell (Å)	2.07–2.00	2.07–2.00	1.76–1.70	2.28–2.20	2.28–2.20	2.28–2.20
No. of unique reflections	24461	24368	57187	39363	39387	39402
No. of observations	260714	166922	295829	294163	222902	223513
Completeness (%)	99.9 (99.9)	99.6 (99.8)	99.0 (99.9)	97.3 (99.4)	97.0 (99.5)	97.1 (99.6)
Mosaicity (°)	0.4	0.5	0.344	0.5	0.5	0.5
R_{merge}‡	0.053 (0.226)	0.068 (0.240)	0.051 (0.188)	0.111 (0.276)	0.102 (0.272)	0.101 (0.324)
$I/\sigma(I)$	44.3 (11.1)	34.2 (7.8)	25.0 (8.3)	8.2	8.2	7.6

† Matthews coefficients V_M (Matthews, 1968) and solvent content were calculated using the *CCP*4 program *MATTHEWS_COEF* (Collaborative Computational Project, Number 4, 1994). ‡ $R_{merge} = \sum(|I_j - \langle I\rangle|)/\sum\langle I\rangle$, where I_j is the observed intensity of reflection j and $\langle I\rangle$ is the average intensity of multiple observations.

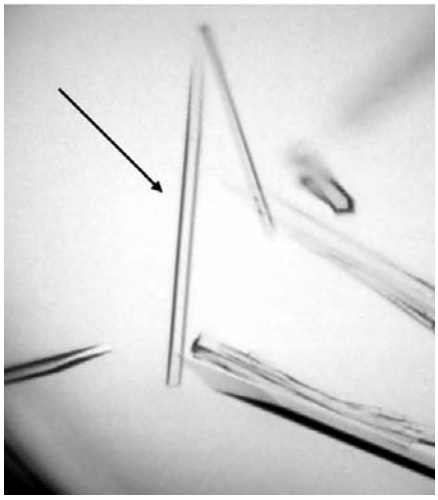

Figure 3
Typical Orn crystals obtained from sodium citrate. The crystal marked with an arrow in the center of the panel has dimensions of approximately 0.70 × 0.035 × 0.025 mm.

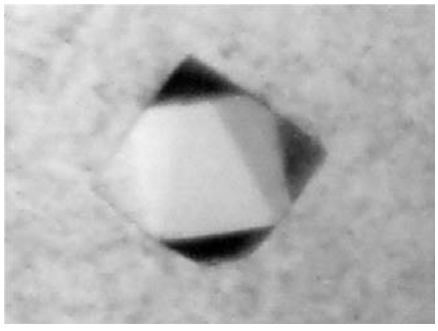

Figure 4
A typical Orn crystal (~0.15 × 0.15 × 0.15 mm) obtained using sodium acetate as a precipitant.

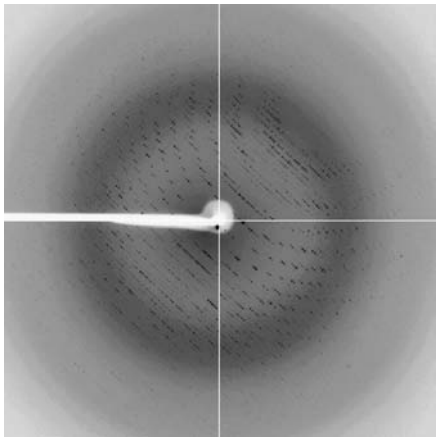

Figure 5
Diffraction from a cryocooled SeMet-labeled Orn crystal (sodium citrate condition), taken at the X8-C beamline at the NSLS (2 min exposure). The outer edge of the image plate is at 2 Å resolution.

3. Results

Orn crystals grown from ammonium sulfate only diffract to about 3.5 Å resolution. Significantly higher resolution diffraction was detected from crystals obtained with sodium citrate. These crystals are rod-shaped and frequently grow as clusters and are often marred by twinning. Crystals grown with sodium citrate were cryoprotected by soaking in four successive steps over a period of 4 min in a substitute mother liquor containing 2.5, 5, 7.5 and 10% glycerol.

Several complete data sets have been collected. A three-wavelength MAD data set was collected from the SeMet-Orn crystal (Table 1; Fig. 5). This crystal was grown over a period of one month from a droplet containing 2 µl of SeMet-Orn at 10 mg ml^{-1} and an equal volume of reservoir solution (1.5 *M* sodium citrate, 50 m*M* Tris pH 7.5). The 20 selenomethionine sites in the asymmetric unit (five per Orn monomer) were identified by *SOLVE* and used to phase this MAD data set to a figure of merit of 0.54 (at 2.5 Å). Solvent flattening by *RESOLVE* extended the figure of merit to 0.7 (at 2.5 Å; 0.64 at 2.2 Å). Based on the correlation between anomalous differences at the three wavelengths, useful experimental phases extend to about 2.2–2.4 Å.

As noted above, several of the Orn crystals grown with sodium citrate appear to be visibly (epitaxially) twinned. Initial screening of crystals with no apparent

epitaxial twinning occasionally resulted in diffraction images which contained a weaker set of reflections outside the main set being indexed. Such twinning is likely being exacerbated by the similar unit-cell parameters ($a \simeq b$, see Table 1) in our orthorhombic space group, which may thus emulate tetragonal space groups. Indeed, the lattice-distortion values obtained during data indexing (*DENZO*; Otwinowski & Minor, 1997) for both orthorhombic as well as tetragonal lattices are below 1%. Efforts were made during indexing to exclude any weaker set of reflections resulting from twinning. In addition, all diffraction data were checked for pseudo-merohedral twinning (the orthorhombic space groups have no twinning operators for true merohedral twinning) using common statistical tests. These include the cumulative distribution plots and moments of the spot intensities, which have different expected values for twinned and untwinned data (Chandra *et al.*, 1999; *TRUNCATE* and *DETWIN* programs from the *CCP*4 package).

Interestingly, when Orn crystals were grown in the presence of manganese (2 m*M* $MnCl_2$) with sodium citrate as the precipitant, we obtained crystals with a markedly different morphology than those shown in Fig. 3. These crystals (Mn-SeMet-Orn) are nearly cubic in perspective and show no visible signs of twinning. Furthermore, these Mn-SeMet-Orn crystals grow to a comparatively large size over several months and diffract to beyond 2.0 Å.

A two-wavelength MAD data set was collected from an Mn-SeMet-Orn crystal grown in the presence of 2 m*M* $MnCl_2$ using 1.55 *M* sodium citrate as the precipitant (Table 1). Diffraction extended to 2.0 Å, although the correlation of the anomalous differences suggested that data beyond approximately 2.3 Å did not contribute greatly to the phasing information. Assuming one dimer in the asymmetric unit, only four of the expected ten selenium sites were located using *SOLVE*. The overall figure of merit from *SOLVE* using data to 2.2 Å is 0.44, which was improved to 0.59 through solvent flattening using *RESOLVE*.

Oligoribonuclease structures solved from both these data sets (results not shown; Fiedler, Zuo and Malhotra, in preparation) showed no metals bound to the protein even though DEDD-family exonuclease catalytic sites have two metal-binding sites. This is likely to be because of the metal-chelating properties of sodium citrate, which was used as the precipitant for the SeMet-Orn and Mn-SeMet-Orn crystals. A similar lack of metal binding was seen even when we soaked Orn crystals obtained with sodium citrate in buffers containing $ZnSO_4$ (2–10 m*M*) before data collection (data not shown).

Data were also collected from Orn crystals obtained with sodium acetate as a precipitant. These crystals are hexagonal in morphology and data were collected from a crystal that was soaked in 8.5 m*M* zinc acetate and 3 m*M* ApUp for 1 h and carefully washed before being cryocooled (Zn-ApUp-Orn; Table 1). Although model building and refinement of the structure of oligoribonuclease from this data set is currently in progress, there appears to be excellent metal binding in these crystals (Yuhong Zuo & Arun Malhotra, unpublished results). This was also corroborated by fluorescence-energy scans on this crystal, which showed a strong peak at 1.2807 Å (data not shown), close to the zinc X-ray absorption *K* edge at 1.2837 Å.

We thank Leonid Flaks at the X8-C beamline, Dieter Schneider at the X12-B beamline and Anand Saxena at the X12-C beamline, National Synchrotron Light Source, Brookhaven National Laboratory for assistance with data collection. Murray Deutscher provided clones and valuable suggestions. This work was supported by Florida Biomedical Research Foundation grant BM030 (AM) and National Institutes of Health grant GM69972 (AM). YZ was supported in part by an American Heart Association Florida/Puerto Rico Affiliate postdoctoral fellowship (0325296B).

References

Bateman, A., Birney, E., Cerruti, L., Durbin, R., Etwiller, L., Eddy, S. R., Griffiths-Jones, S., Howe, K. L., Marshall, M. & Sonnhammer, E. L. (2002). *Nucleic Acids Res.* **30**, 276–280.
Bradford, M. M. (1976). *Anal. Biochem.* **72**, 248–254.
Breyer, W. A. & Matthews, B. W. (2000). *Nature Struct. Biol.* **7**, 1125–1128.
Carpousis, A. J., Vanzo, N. F. & Raynal, L. C. (1999). *Trends Genet.* **15**, 24–28.
Chandra, N., Acharya, K. R. & Moody, P. C. E. (1999). *Acta Cryst.* D**55**, 1750–1758.
Coburn, G. A. & Mackie, G. A. (1999). *Prog. Nucleic Acid Res. Mol. Biol.* **62**, 55–108.
Collaborative Computational Project, Number 4 (1994). *Acta Cryst.* D**50**, 760–763.
Datta, A. K. & Niyogi, S. K. (1975). *J. Biol. Chem.* **250**, 7313–7319.
Deutscher, M. P. (1993). *J. Bacteriol.* **175**, 4577–4583.
Deutscher, M. P. & Li, Z. (2001). *Prog. Nucleic Acid Res. Mol. Biol.* **66**, 67–105.
Donovan, W. P. & Kushner, S. R. (1986). *Proc. Natl Acad. Sci USA*, **83**, 120–124.
Doublié, S. (1997). *Methods Enzymol.* **276**, 523–530.
Ghosh, S. & Deutscher, M. P. (1999). *Proc. Natl Acad. Sci. USA*, **96**, 4372–4377.
Hamdan, S., Carr, P. D., Brown, S. E., Ollis, D. L. & Dixon, N. E. (2002). *Structure*, **10**, 535–546.
Hollams, E. M., Giles, K. M., Thomson, A. M. & Leedman, P. J. (2002). *Neurochem. Res.* **27**, 957–980.
Jancarik, J. & Kim, S.-H. (1991). *J. Appl. Cryst.* **24**, 409–411.
Kennell, D. (2002). *J. Bacteriol.* **184**, 4645–4657.
Kohara, Y., Akiyama, K. & Isono, K. (1987). *Cell*, **50**, 495–508.
Koonin, E. V. (1997). *Curr Biol.* **7**, R604–R606.
Matthews, B. W. (1968). *J. Mol. Biol.* **33**, 491–497.
Nguyen, L. H., Erzberger, J. P., Root, J. & Wilson, D. M. III (2000). *J. Biol. Chem.* **275**, 25900–25906.
Otwinowski, Z. & Minor, W. (1997). *Methods Enzymol.* **276**, 307–326.
Steitz, T. A. (1999). *J. Biol. Chem.* **274**, 17395–17398.
Terwilliger, T. C. (2000). *Acta Cryst.* D**56**, 965–972.
Terwilliger, T. C. & Berendzen, J. (1999). *Acta Cryst.* D**55**, 849–861.
Van Duyne, G. D., Standaert, R. F., Karplus, P. A., Schreiber, S. L. & Clardy J. (1993). *J. Mol. Biol.* **229**, 105–124.
Yu, D. & Deutscher, M. P. (1995). *J. Bacteriol.* **177**, 4137–4139.
Zhang, X., Zhu, L. & Deutscher, M. P. (1998). *J. Bacteriol.* **180**, 2779–2781.
Zuo, Y. & Deutscher, M. P. (2001). *Nucleic Acids Res.* **29**, 1017–1026.